Journal of Harbin Institute of Technology(New series)
哈尔滨工业大学学报(英文版)
ISSN 1005-9113,CN 23-1378/T

《Journal of Harbin Institute of Technology(New series)》网络首发论文

题目： Review: Progress in the Preparation of Iron Based Magnetic Nanoparticles for Biomedical Applications

作者： Yu Mao，Yan Li，Ning Gu

收稿日期： 2019-02-25
网络首发日期： 2019-04-04
引用格式： Yu Mao，Yan Li，Ning Gu．Review: Progress in the Preparation of Iron Based Magnetic Nanoparticles for Biomedical Applications[J/OL]．Journal of Harbin Institute of Technology(New series).
http://kns.cnki.net/kcms/detail/23.1378.T.20190404.1057.002.html

Published online：2019-04-04 16:15:08
URL：http://kns.cnki.net/kcms/detail/23.1378.T.20190404.1057.002.html

Journal of Harbin Institute of Technology (New Series)
DOI：10.11916/j.issn.1005-9113.2018004

Review: Progress in the Preparation of Iron Based Magnetic Nanoparticles for Biomedical Applications

*Yu Mao, Yan Li and Ning Gu**

(State Key Laboratory of Bioelectronics, Jiangsu Key Laboratory for Biomaterials and Devices, School of Biological Sciences and Medical Engineering, Southeast University, Nanjing 210096, China)

Abstract：With unique physical properties, chemical properties, and biological effects, magnetic nanomaterials are important functional materials in many fields. In the past decades, iron based magnetic nanomaterials have attracted much attention in the biomedicine field due to their superior magnetic properties and great potential in biomedical applications. In particular, magnetic iron oxide nanoparticles (MIONPs) have been playing a crucial role in the biomedicine field because of their diagnostic and therapeutic functions. Meanwhile, MIONPs are benign, low toxic, biocompatible, and biodegradable, so they are the only inorganic magnetic nanomaterials approved by the U.S. Food and Drug Administration (FDA) for clinical use at present. In this review, we mainly introduce the progress in the preparation of iron based magnetic nanomaterials for biomedical applications, including pure iron nanoparticles, iron-based alloy nanoparticles, and MIONPs, with a focus on MIONPs. Also, we summarize the preparation methods of MIONPs and point out the importance of their developments.

Keywords: iron-based magnetic nanomaterials; biomedical applications; MIONPs; diagnostic and therapeutic functions; preparation methods

CLC number: TB34 **Document code：A**

1 Introduction

As important functional materials, magnetic nanomaterials are extensively applied in data storage, energy storage, biomedicine, and catalysis because of their unique physical properties, chemical properties, and biological effects[1]. Transition elements including iron (Fe), cobalt (Co), and nickel (Ni) exhibit ferromagnetism, and the nanomaterials based on them usually have superior magnetism. Co NPs and Ni NPs have been proved to be toxic for biomedical applications. When the concentration of Co NPs is greater than 10^{12} particles/ml, they will be cytotoxic to the most of the cells[2]. As to Ni NPs, numerous studies have demonstrated that they have genotoxicity, oxidative stress, and pro-inflammatory responses, and they can even cause cell death and cancers in vivo[3]. Iron is the fourth most plentiful element on the earth[4], which is an important metallic element in human body that participates in many essential life activities. Bulk iron is ferromagnetic with a high magnetization of 218 emu/g, while iron based magnetic NPs smaller than 20 nm are usually superparamagnetic[5]. Therefore, pure metal, alloy, and oxide nanomaterials based on iron have attracted much attention in the biomedicine field due to their superior properties and biological effects[6-7]. The excellent magnetism enables iron based magnetic nanomaterials to exhibit various diagnostic and therapeutic functions, such as magnetic resonance imaging (MRI)[8-9], tumor hyperthermia[10], cell labeling[11], target drug delivery[12], and cell sorting[13]. Moreover, magnetic iron oxide nanoparticles (MIONPs) have peroxidase-like activity, which was first discovered in 2007[14], and later, more enzyme-like

Received 2019-02-25.
Sponsored by the National Natural Science Foundation of China (Grant Nos. 51832001, 31800843), the National Key Research and Development Program of China (Grant No. 2017YFA0104301), and the Collaborative Innovation Center of Suzhou Nano Science and Technology (Grant No. SX21400213).
* Corresponding author. Distinguished Professor of Yangtze River Scholar and Winner of the National Science Fund for Distinguished Young Scholars.
E-mail: guning@seu.edu.cn

activities such as catalase activity[15-16] were revealed. Because of these enzyme-like activities, MIONPs are utilized in a series of novel biomedical applications, including immunoassay, pathogen detection, anti-bacteria, and the modulation of cellular oxidative stress. As the first and the most typical nanozyme, MIONPs have initiated the discovery of enzyme-like activities of many other inorganic nanomaterials[17-18]. If used as a platform with grafted functional biological moieties or drugs, MIONPs can realize the integration of several functions on one nanoparticle[1,19].

The properties of magnetic nanomaterials mostly depend on their compositions[9,20], structures[21-22], sizes[8,22], and morphologies[23-26]. An appropriate preparation method is the key to make the magnetic nanomaterials with superior or adjustable properties. The synthesis routes of iron based magnetic nanomaterials can be roughly classified into two categories according to the types of solvents. The first was carried out in aqueous solution via co-precipitation method[27-28], hydrothermal method[29-30], electrochemical method[31-32], etc. The other was performed in organic medium via high-temperature decomposition method[33-34], sol-gel method[35-36], polyol method[37-38], micro-emulsion method[39-41], etc. Furthermore, some external physical fields such as visible light[42-43], ultrasonic[44-45], microwave[46-47], static magnetic field[48-49], and alternating magnetic field[50-51] have been studied to assist the preparation of iron based magnetic nanomaterials. Up to now, plenty of literature has reported the preparation, functionalization, and biomedical application of iron based magnetic nanomaterials. In this review, the synthesis of iron based magnetic nanomaterials, including pure iron, iron based alloy, and iron oxides, is summarized starting from the formation mechanism of nanoparticles. The preparations, modifications, functionalizations, and biomedical applications of iron based magnetic nanoparticles are introduced in Fig.1.

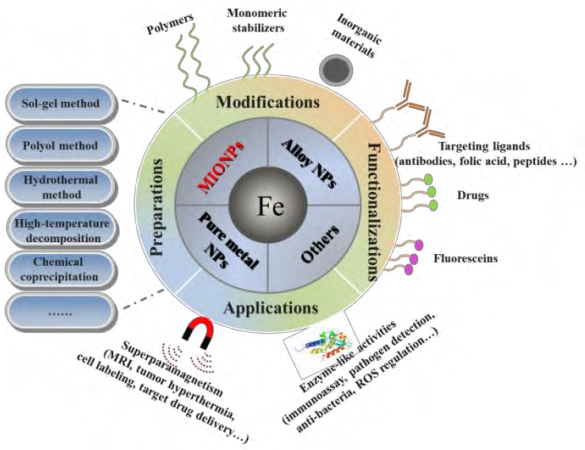

Fig. 1 Preparations, modifications, functionalizations, and applications of iron based magnetic nanoparticles

2 Formation Mechanism of Nanoparticles

Understanding the formation mechanism of NPs is necessary for their controlled synthesis. The specific formation mechanism of magnetic NPs is not fully clear, because their reaction process involves complex reaction kinetics[7,52]. LaMer's mechanism[53] is a classical theory which is often used to describe the formation process of NPs. As LaMer model[54] depicts (Fig.2), the formation process of NPs is divided into three stages on the basis of the time evolution of monomer concentration in the synthetic solution. At stage I, the monomer concentration continuously increases and exceeds the critical supersaturation concentration (C_s), approaching the critical nucleation concentration (C_{min}). At stage II, when the monomer concentration surpasses C_{min}, burst nucleation takes place by consuming monomers and the supersaturation is rapidly relieved. At stage III, when the monomer concentration passes below C_{min}, no new nuclei are formed. The as-formed nuclei start to grow by consuming residual monomers until the monomer concentration drops to a sufficiently low level. In fact, the other form of growth called Ostwald ripening also takes place at stage III[54-55]. The small and unstable particles will partially digest and support the growth of larger particles driven by the thermodynamic factors.

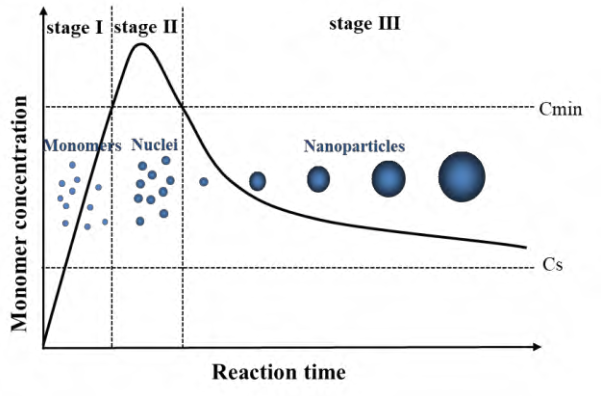

Fig. 2 LaMer model of the nucleation and growth processes for NPs

Nucleation is the first and the most important process of the formation of NPs, which determines the crystal structure and size distribution of the final particles. The most widely used classical nucleation theory presumes that the long-range structure of crystal is constructed by the ordered stacking of monomers[56]. This classical theory is originally derived from the process of vapor condensing into liquid, so it has limitations to explain the nucleation in solution. In order to explain the nucleation of crystals from supersaturated solutions more appropriately, a non-classical two-step nucleation model has been put forward. This model assumes that the solute molecules first construct a cluster, and then an ordered structure forms by the rearrangement of molecules. The two-step nucleation model is originated from the protein crystallization and is applicable to most of the crystalline phenomena in the solution[56]. Due to the development of advanced characterization techniques, the observations of nucleation and growth processes are becoming more and more real-time and visual. For example, Baumgartner et al.[57] studied the nucleation and growth of Fe_3O_4 NPs based on the co-precipitation reaction in solution by using the high-resolution cryogenic transmission electron microscopy (cryo-TEM). Their observations showed that disordered primary clusters/particles with the size of 1-2 nm first formed from a gel-like network structure, and then the Fe_3O_4 crystal formed and grew by the fusion and accretion of primary clusters/particles. This growth pattern is very similar to the way that particles grow through the accretion of monomers, which has been depicted in the classical nucleation theory. The correlative thermodynamic theory analyses of this study indicates that the occurrence of classical or non-classical nucleation is determined by the thermodynamic free energies of primary particles, amorphous bulk phases, and crystalline bulk phases.

The growth rate of nuclei is relatively slow compared with the rate of nucleation, so the growth process can be more easily controlled by the regulation of aging temperature and duration. As introduced above, the formed nuclei will grow via the accretion of monomer or the dissolution-crystallization of small particles. In order to prepare NPs with narrow particle size distribution, it is essential to keep the nuclei burst forming in a short time and growing at a uniform rate. In the preparation process of MIONPs via high temperature decomposition, the oleate ligands dissociate from the precursor $Fe(oleate)_3$ at two different temperatures, which correspondingly separates the burst nucleation and time-dependent growth processes at two different temperatures. Therefore, the monodisperse MIONPs are synthesized successfully[33]. If the nucleation does not take place uniformly in a short time, the followed Ostwald ripening or additional nucleation will result in the coexistence of particles with great difference. In addition to ensure the nucleation as uniform as possible, an extending LaMer mechanism[54] was also designed to avoid the Ostwald ripening. In this extending process, the precursors were continuously added to sustain the growth of NPs, and the size and shapes of the final NPs were controlled in a narrow dispersity.

The shape control of NPs on the basis of the thermodynamic and kinetic controls of growth was studied[58-59]. According to the surface energy sequence $\gamma(111) < \gamma(100) < \gamma(110) < \gamma(220)$ of face-centered-cubic structure, the most stable exposed

facet of MIONPs should be {111} facets. However, the exposed facets and the shape of the MIONPs are mainly dependent on their growth rate along different crystal orientations. MIONPs with different shapes such as sphere, octahedron, octapod-star, and cube are successfully controlled to be formed with the assist of surfactants. Feld et al.[59] studied the shape transition of MIONPs via the thermal decomposition of iron oleate with different reaction conditions including molar ratios of Fe and oleic acid, 1-octadecene dilutions, and reaction time. Oleic acid can strongly stabilize the {100} facets of the initially formed tiny cubic MIONPs and make the MIONPs preferentially grow along the <111> directions, so the shape of octapod-star formed in the initial reaction phase. In this kinetically controlled growth phase, the rate of the monomers deposited on the as-formed NPs was higher than their diffusion rate on the surface of NPs. When the monomer was exhausted in the later phase, the atoms began to diffuse to the edges and side facets of the octapod-star driven by thermodynamics, and promoted the final formation of cubic MIONPs.

3 Synthesis of Pure Fe Magnetic Nanoparticles

Pure Fe NPs are usually prepared by the thermal decomposition or chemical reduction of the precursor compounds of iron. Amorphous and body centered cubic (bcc) are two relatively stable structures of Fe NPs, while the face centered cubic Fe (fcc-Fe) is thermodynamically unstable. Zhang et al.[60] synthesized bcc-Fe NPs and amorphous Fe (amor-Fe) NPs via the thermal decomposition of $Fe(CO)_5$. In the presence of halide ions (Cl^- or Br^-), the growth of Fe NPs was restricted and the bcc-Fe NPs were preferably formed, while the amor-Fe NPs would form quickly without the addition of halide ions (Fig.3). The size of bcc-Fe NPs can be controlled by adjusting the amounts of precursor $Fe(CO)_5$ and stabilizing agent oleylamine. Ling et al.[4] designed a thermodynamically governed synthetic route and successfully synthesized 5-13 nm fcc-Fe NPs, which nucleated and grew into triangular facets enclosed icosahedral morphology so as to minimize the surface energy. It can be concluded that Fe NPs with different structures can be prepared via the process control of different methods, and their size, crystallinity, and magnetic properties can be modulated by choosing different ligands or changing reaction conditions[61].

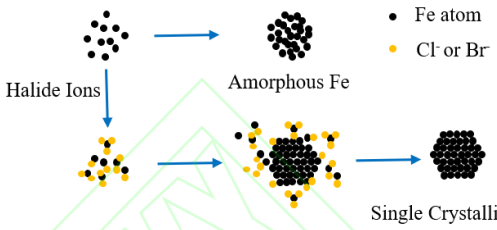

Fig. 3 Schematic of the formation processes of amorphous Fe NPs and bcc-Fe NPs

Bare Fe NPs are not safe enough to be used for medicine, because they can easily aggregate, which induces the thrombus, and they are easily oxidized and extremely reactive to form dangerous radicals[62]. It is difficult to produce a stable Fe NPs aqueous dispersion for biomedical applications without a robust surface protection (such as polymer, silver, gold, and iron oxide). Monodisperse Fe_3O_4 encapsulated Fe NPs were synthesized through the pyrolysis of $Fe(CO)_5$ and a controlled oxidization of the surface[5]. The crystalline Fe_3O_4 shell increased the chemical stability and dispersibility of Fe NPs greatly. Once modified with functional molecules[63], the Fe@Fe_3O_4 NPs can be used for the MRI and magnetic fluid hyperthermia of tumor simultaneously. Lu et al.[64] synthesized the Fe NPs by reducing $FeCl_2$ precursor, and then they coated the Fe NPs with Ag shell by a second reduction process. The as-prepared Fe@Ag core-shell NPs possess sensitive plasmonic properties and adjustable magnetism. Superparamagnetic Fe@Au core-shell NPs were prepared by the reverse micelle method using $FeSO_4$ as iron precursor, $HAuCl_4$ as gold precursor, and $NaBH_4$ as a reductant[62]. The gold shell of Fe@Au NPs can strongly bind with anti-cancer drug doxorubicin by

amine groups, so they can be used for the targeted delivery and release of drugs under the effect of an external magnetic field.

4 Synthesis of Iron-Based Alloy Magnetic Nanoparticles

In order to get a more superior magnetism, iron-based alloy magnetic NPs are prepared by doping different elements, and the doping of MIONPs will be introduced in the next section. The iron-based alloy magnetic NPs exhibit different properties from pure Fe NPs because of the synergistic effects of different elements, and they hold potentials in biomedical applications. Cubic $Fe_{70}Co_{30}$ NPs with 8 nm edge length were prepared by physical gas condensation. In this process, the FeCo alloy with Fe:Co atomic composition of 70:30 was used as a sputtering source and argon gas served as both sputtering gas and carrier gas. The as-prepared $Fe_{70}Co_{30}$ NPs were modified by the existing polyvinylpyrrolidone on the glass slide and they had high magnetization (~226 emu/g) which was much higher than that of the bulk magnetite (~127 emu/g Fe). If used as hyperthermia agent, they will exhibit great magnetic heat effect[65]. Spherical FeCo NPs (20-30 nm) with a similar magnetization (~221 emu/g) to cubic $Fe_{70}Co_{30}$ NPs were synthesized on a large-scale via a modified polyol synthesis. The precursors iron chloride and cobalt acetate were heated at 200 ℃ in the ethylene glycol, which served as solvent, reductant, and surfactant in the presence of NaOH. The magnetization of bare FeCo NPs will decrease if they are exposed to air for a long time because of oxidization[66]. FeCo NPs coated with graphitic shell (FeCo@GC) were prepared by scalable chemical vapor deposition method. As reported, they have good effects on the labeling and T_2-MRI of mesenchymal stem cells (hMSCs) and the long-lasting T_1-MRI of vascular, due to their high transverse relaxation value r_2 and longitudinal relaxation value r_1. In addition, the FeCo@GC NPs possess high near-infrared (NIR) optical absorbance, indicating that they can also be used for the photothermal therapy of tumor. No obvious toxicity was observed in vivo or in vitro assays of FeCo@GC NPs[9]. Another kind of alloy magnetic NPs, FePt NPs, was synthesized by the thermal decomposition of $Fe(OEt)_3$ and $Pt(acac)_2$. The FePt NPs exhibit a higher transverse shortening effect than MIONPs, so they are expected to be good candidates of T_2-weighted MRI contrast agent[67-68]. In addition to MRI contrast effect, FePt NPs also show good effect in CT imaging and tumor hyperthermia. Compared with Fe NPs, FePt NPs is chemically stable and oxidation-resistant, while the bare FePt NPs show cell cytotoxicity on a relatively high concentration[67]. Cysteamine modified FePt NPs prepared by polyol method present excellent biocompatibility and hemocompatibility, so they are expected to be used as MRI/CT dual modal imaging contrast agent, and the ultra-small FePt NPs with the size of 3 nm can even be used for the multimodal imaging of brain[69]. Yang et al.[70] prepared Fe_5C_2 NPs by the hot injection strategy at 623 K using $Fe(CO)_5$ as precursor, octadecylamine as both solvent and surfactant, and cetyltrimethylammonium bromide (CTAB) as inducing agent. The bromide is vital to the crystallization of originally formed Fe NPs and finally generated Fe_5C_2 NPs. The as-synthesized Fe_5C_2 NPs have high saturation magnetization (~125 emu/g), which makes them possess excellent T_2 MRI contrast effect. Meanwhile, the Fe_5C_2 NPs have an amorphous carbon shell which protects them from oxidation and endows them with high absorption in NIR. Thus, the carbon-coated Fe_5C_2 NPs can realize multi-functions including MRI, photothermal therapy (PTT), and photoacoustic tomography (PAT). Under certain concentrations, the carbon-coated Fe_5C_2 NPs did not show significant cytotoxicity[71-72]. As mentioned above, some iron based alloy magnetic NPs exhibit superior magnetic properties, so they are expected to be more effective candidates for biomedical applications.

However, same as pure Fe NPs, the easy oxidation and potential toxicity usually limit their biomedical applications.

5 Synthesis of MIONPs

MIONPs with an appropriate surface coating are benign, low toxic, biocompatible, and biodegradable, so they can be injected into human body and incorporated into human body metabolism[73]. MIONPs have drawn much attention from researchers in the past decades, and they are the most widely used magnetic nanomaterials in the biomedicine field at present. Magnetite (Fe_3O_4) and maghemite (γ- Fe_2O_3) are two important magnetic minerals belonging to iron oxides family, which constitute MIONPs as usually mentioned in the biomedicine fields because of their unique magnetic properties. As aforementioned, many methods can be used to prepare MIONPs, so we will introduce several typical methods including chemical co-precipitation methods, solvothermal methods, and high-temperature decomposition methods in this section.

5.1 Chemical Co-Precipitation Method

Among all the methods, chemical co-precipitation method is the simplest way to prepare hydrophilic MIONPs on a large scale, which is commonly used to prepare MIONPs for biomedical applications. Numerous commercially available MIONPs drugs, such as Feridex© and Resovist©, are prepared by this method. Since the co-precipitation reaction is carried out in the aqueous solution, it is cost-effective and environmentally friendly. Meanwhile, their products are water disperse and can be directly used for biomedicine without a complicated ligand exchange treatment. The co-precipitation reactions of Fe_3O_4 formation usually proceed via the hydrolysis and condensation of ferrous and ferric ions in the aqueous solution at a pH between 8 and 14, as expressed in Eq. (1)[27,74].

$$Fe^{2+} + 2Fe^{3+} + 8\ OH^- = Fe_3O_4 + 4H_2O \quad (1)$$

There are several challenges for the preparation of MIONPs through the co-precipitation method. First, the reaction process involves complicated hydrolysis reactions and various hydrolytic byproducts including the hydroxides, oxyhydroxides, and oxides of Fe which can be generated in the hydrolysis process (Fig.4), so it requires a careful pH adjustment of the reaction medium[75]. Second, the nucleation and growth processes of MIONPs are not separated in the co-precipitation synthesis, which limits the control of their size distribution. Third, the co-precipitation reaction proceeds in the polar aqueous medium and the reaction temperature is usually not above 90 ℃, so their products have irregular shapes and low crystallinity.

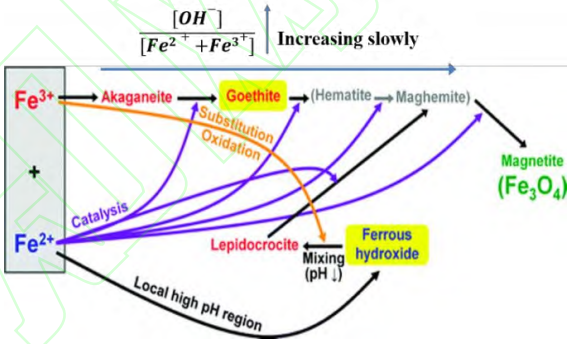

Fig. 4 Formation pathways of MIONPs prepared via co-precipitation method (reproduced with permission[75], Copyright 2012, American Chemical Society)

Since Massart[76] first put forward the co-precipitation method, a lot of researchers have studied the co-precipitation reaction with various reaction conditions such as pH, reaction temperature, ion concentration, nature of salts, type of alkali, and ion strength.[74,77-79] In order to overcome the abovementioned challenges, some improved co-precipitation methods have been applied to prepare MIONPs. Li et al.[27] prepared MIONPs by the rapid injection of iron salts solution and ammonia solution into the refluxing hot polymer aqueous solution. The products prepared by this method exhibit narrow size distribution and high crystallinity compared with standard co-precipitation. Since the rapid injection of all the precursors will yield a high supersaturation

concentration in a short time, the burst nucleation is faster and can be better separated from the growth process of particles compared with dropwise addition. Shen et al.[28] synthesized a series of poly (acrylic acid) (PAA) coated extremely small MIONPs (ES-MIONPs, smaller than 5 nm) with different sizes through a similar rapid hot injection method. The hot injection method improves the particle size distribution by accelerating the nucleation. The magnetization of the ES-MIONPs is very low because of the surface spin-canting effect, while they have good T_1-MRI effects due to the large number of surface ions. As a kind of T_1-weighted MRI contrast agent, ES-MIONPs show better biosecurity and have longer internal circulation time than traditional Gd-chelates. The study also constructed a drug delivery system based on the ES-MIONPs, which lowered the nonspecific uptake of ES-MIONPs by combining the passive and active tumor targeting and realized the pH-responsive release of anticancer drugs at the same time. The drug delivery system was applied to the T_1-weighted MRI and chemotherapy of integrin-expressing tumors bearing mice effectively. The T_1-weighted MRI contrast effect of MIONPs is mainly induced by the interaction between the surface electron spins and the protons of surrounding water molecules, while the T_2-weighted MRI contrast effect is strongly associated with the magnetic properties of MIONPs. Therefore, compared with ES-MIONPs, MIONPs with larger size and higher magnetization are usually used for T_2-weighted MRI[80-81]. MIONPs with particle sizes ranging from 7.5 nm to 416 nm were prepared via two kinds of chemical co-precipitation methods[82-83]. A typical strategy was used to synthesize the 7.5 nm and 13 nm MIONPs by dropping ammonia aqueous solution into the solution of precursors $FeCl_3$ and $FeSO_4$ until their PH reached 9. The preparation of larger MIONPs usually adopts the oxidation co-precipitation method. In the oxidation co-precipitation reaction process, only Fe (Ⅱ) salts were used as precursors, and the solution of Fe (Ⅱ) salts first formed $Fe(OH)_2$ gels in the presence of base. Then, Fe (Ⅱ) was partly oxidized to Fe (Ⅲ) by the oxidizing agent KNO_3 and they precipitated as the form of magnetite during the long time aging at 90 ℃. The size of the large MIONPs was controlled by regulating the concentration of the reaction solution. Oleic acid coated MIONPs were synthesized through a novel oxidation co-precipitation method in a mixed solvent of H_2O and dimethyl sulfoxide (DMSO) heating at 140 ℃. In this process, $(NH_4)_2Fe(SO_4)_2•6H_2O$ or $FeSO_4•7H_2O$ was used as a precursor, which was partially oxidized by DMSO and precipitated to form the ES-MIONPs in the presence of alkaline tetramethylammonium (TMAOH) and surfactant oleic acid. The reaction temperature is relative low compared with the high-temperature decomposition method which is usually used to prepare oleic acid coated MIONPs[84-85]. In order to speed up the mix of reaction solutions and minimize the local variations of concentration and temperature during the co-precipitation process, microfluidic reactors were designed and applied to the preparation of MIONPs. Hassan et al.[86] designed a millimetric coaxial continuous flow device as shown in Fig.5 (a). The TMAOH solution first flows into the outer capillary through the entrance Q_{out} and wets the polydimethylsiloxane (PDMS) wall. Then the mixed solution of Fe (Ⅱ) and Fe (Ⅲ) flows into the stream of TMAOH solution through the inner capillary. The reaction solutions mix and react under the laminar flow state, and the TMA^+ adsorbs on the surface of MIONPs to enhance their colloidal stability. A capillary-based droplet reactor was designed by Kumar et al.[87] as shown in Fig.5 (b). The NH_4OH aqueous solution and the mixed aqueous solution containing Fe (Ⅱ), Fe (Ⅲ), and dextran encounter at the intersection of capillaries, and the reaction solution are divided into a series of droplets by the immiscible carrier liquid octadecene. The droplets are nearly identical and they flow at a constant linear velocity, ensuring that the reaction

solutions can mix and react at a uniform condition. Therefore, the obtained MIONPs exhibit relatively narrow particle size distribution compared with bulk synthesis, and the continuous microfluidic reactors can prepare MIONPs automatically and reproducibly.

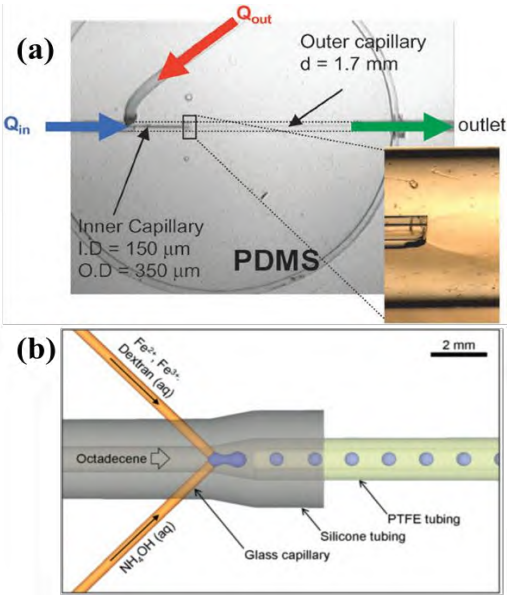

Fig. 5 Schematic of (a) a coaxial flow device operating under a laminar regime (reproduced with permission[86], Copyright 2008, Royal Society of Chemistry); (b) a capillary-based droplet reactor (reproduced with permission[87], Copyright 2012, Royal Society of Chemistry)

To improve the heating state of co-precipitation reactions, Chen et al.[50,88] utilized alternating-current magnetic field (ACMF) induced heat to assist the synthesis of ferumoxytol, which is a kind of MIONPs that has been approved for clinical application in the USA. The solution of polyglucose sorbitol carboxymethyl ether (PSC, a kind of modified dextran) was mixed with precursor solution containing ferrous chloride and ferric chloride. When the alkaline ammonia aqueous solution was dropped into the mixed solution, the nuclei of magnetite NPs started to form. The as-formed nuclei can generate heat by themselves uniformly and rapidly under a high frequency ACMF based on the Neel Relaxation and Brown Relaxation [82,89]. The whole reaction was carried out in a high frequency ACMF without an external heating, and the heat generated by the particles themselves could support their further growth and crystallization. After an oxidation process, the ferumoxytol composed of a γ-Fe_2O_3 core and a PSC shell was prepared. This innovative heating strategy avoids the non-uniformity and time-consumption of the traditional heating modes, which mainly conduct heat from outside to inside through solvent. The products prepared by this method exhibit better properties than ferumoxytol which is prepared by traditional heating mode on particle size distribution, crystallinity, and magnetism. As far as we know, such heating mode named magnetically internal heating method is the first time to be put forward. Further study[51] highlights the effect of magnetically internal heating by adding hydro-cooling to shield the heat of solvent at the original stage. The hydro-cooling condition can control the increase of the temperature of solvent to protect the nucleation from the influence of solvent temperature disturbance and inhibit the growth of MIONPs at the nucleation process. The following growth and ripening processes of nuclei proceed under magnetically internal heating without hydro-cooling to ensure an appropriate aging temperature. After the improvement of this synthesis process, the magnetization and T_2-weighted MRI contrast effect of as-synthesized MIONPs were further enhanced. The comparison between conventional external heating, magnetically internal heating, and hydro-cooling assisted magnetically internal heating methods is shown in Fig.6.

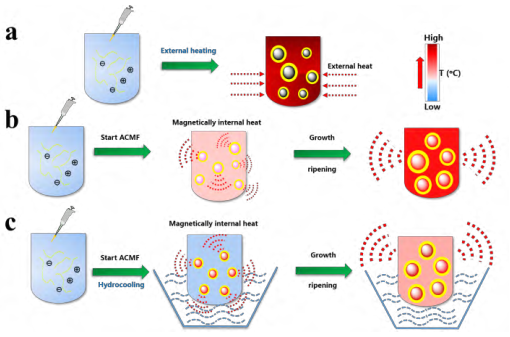

Fig. 6 Schematic of co-precipitation methods based on (a) external heating; (b) magnetically internal heating; (c) hydro-cooling assisted magnetically internal heating (reproduced with permission[51], Copyright 2018, RSC Pub.)

5.2 Solvothermal Method

The preparation of MIONPs via solvothermal methods usually involves the hydrolysis, oxidation, or reduction reactions of ferrous or ferric salts in different solvents. These processes usually proceed with the aid of a high temperature or a high pressure.

5.2.1 Sol-gel Method

The sol-gel method usually contains two stages. The first stage proceeds at a relatively moderate temperature, which mainly involves the hydroxylation, oxidation, and condensation of divalent iron precursors to form a gel of iron oxide. The second stage is the heat treatment at a high temperature to obtain the final crystalline MIONPs. The formation and growth processes of the MIONPs during the nonaqueous sol-gel synthesis are presented in Fig.7.

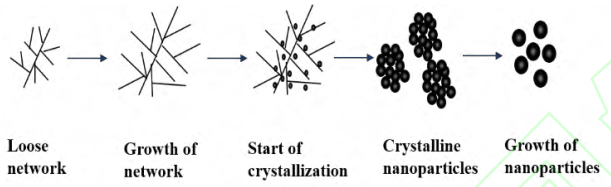

Fig. 7 Formation and growth processes of MIONPs during the sol-gel synthesis

First, precursor molecules partially degenerate with the formation of loose networks. The networks grow as the synthesis proceeds, and then they become compact by releasing the organic compounds and start crystallizing at the same time. Finally, the crystalline MIONPs are formed and grow during the long time heat treatment. By comparing the particles obtained at different stages, the conversion from crystal/amorphous core shell structure to a single crystal is observed. Meanwhile, the initial particles composed of both Fe_3O_4 and γ-Fe_2O_3 convert to pure γ-Fe_2O_3 in the end[35-36]. Sodium dodecyl benzene, a surfactant, can prolong or prevent the gelation of different iron salt solution efficiently, so it can be used to control the growth of MIONPs by being added at different synthesis stages[90]. The structure of MIONPs prepared by sol-gel method is mostly dependent on their drying process. Cui et al.[91] studied the structure switch of MIONPs during the low temperature sol-gel process. They first prepared Fe_3O_4 sol at 78 ℃ using $FeCl_2$•$4H_2O$ as a precursor, ethanol as a solvent, and propylene oxide as a gelation agent, and then they obtained Fe_3O_4 NPs, γ-Fe_2O_3 NPs, and α-Fe_2O_3 NPs by drying the Fe_3O_4 sol in different conditions. Sol-gel method combined with supercritical fluid drying technology is also used to prepare MIONPs. First, the hydrogel and alcogel of $Fe(OH)_3$ are formed in sequence, and then the aerogel of iron oxide is generated through the drying and crystallizing of $Fe(OH)_3$ alcogel in supercritical fluid drying process. Finally, the MIONPs with different phases can be prepared by sintering the aerogel at different temperatures[92]. The preparation of MIONPs via sol-gel method is simple and economical, and the products have good crystallinity resulting from high reaction temperature. The hydroxylation and condensation of iron salts precursors make the MIONPs disperse in the form of a sol, so a post-treatment (such as heat treatment) is necessary for the sol-gel method. Since the purity of their products is strongly influenced by the heat treatment process, the undesired phase (such as α- Fe_2O_3 with weak magnetism) can be usually formed during the sintering process.

5.2.2 Hydrothermal Method

The hydrothermal synthesis of MIONPs proceeds by the hydrolysis of inorganic iron salt in the super-hot (above 100 ℃) water under a high pressure. It is a simple way to synthesize MIONPs in one-pot without multiple step chemical reactions and time-consuming processes[93]. PEI coated magnetite NPs were synthesized via a facile hydrothermal method[94]. The precursor $FeCl_2$•$4H_2O$ was first dissolved in aqueous solution, and then ammonium hydroxide solution was added to the $FeCl_2$ solution and formed a suspension. After stirring for 10 minutes in air to make the divalent iron oxidized, the suspension was mixed with the PEI solution in an autoclave and the hydrothermal process proceeded at 134 ℃ for 3 h under a pressure of 2 bar.

The size of the PEI coated magnetite NPs can be tuned by controlling the ratio of $FeCl_2$•$4H_2O$ to PEI. The PEI modified MIONPs can be further functionalized with many other functional groups. In particular, the PEGylation and acylation will provide the PEI modified MIONPs with good hemocompatibility and cytocompatibility in certain concentration range, so they can potentially be applied to the targeted MRI and therapy of cancer. In the special conditions of hydrothermal synthesis, nonpolar reagents can also be used to modify the products without the use of organic solvents. For example, Takami et al.[95] prepared n-decanoic acid or n-decylamine capped MIONPs by heating the solution of $FeSO_4$ containing n-decanoic acid or n-decylamine at 200 ℃ for 10 min in an autoclave. Neither organic reagents n-decanoic acid nor n-decylamine is miscible with water at room temperature, but they will mix with water in the super-critical hydrothermal environment because of the decrease of the dielectric constant of water. So the MIONPs with different structures and shapes coated with n-decanoic acid or n-decylamine were synthesized successfully without the use of organic solvents. The phases of MIONPs can be controlled by varying the compositions of precursors. For example, α-Fe_2O_3, γ-Fe_2O_3, and Fe_3O_4 will be synthesized if single $FeCl_3$, $FeCl_2$ + $FeCl_3$, or single $FeCl_2$ is correspondingly used as precursor. In this process, ethanol as a co-solvent is mixed in the aqueous solution. The ethanol can attach to the surfaces of the MIONPs through hydrogen bond and inhibit the growth of particles, leading to the smaller size of MIONPs[96]. In addition to the water content of solvents, the precursor concentration[97], reaction time, and reaction temperature[98] are also vital impact factors of the particle size. The hydrothermal synthesis is usually performed in the supercritical or subcritical aqueous solution of inexpensive inorganic salts. The MIONPs prepared by hydrothermal method are usually hydrophilic and have good crystallinity because of the high reaction temperature, but their size and shape uniformities and dispersity seem to be bad.

5.2.3 Polyol Method

To get a uniform size and a high crystallinity, the polyol process is used to synthesize MIONPs, which is usually carried out by the reduction of iron precursor in a polyol solvent at a high reflux temperature. The high-boiling polyol acts as solvent, reducing agent, and coating agent simultaneously, so it correlates to the morphology and colloidal stability of the final products. Cai et al.[37] Prepared Fe_3O_4 NPs by reducing $Fe(acac)_3$ in different polyol solvents including ethylene glycol (EG), diethylene glycol (DEG), triethylene glycol (TREG), and tetraethylene glycol (TEG). The reaction procedures are all similar except the reflux temperatures in relation to each polyol solvent. Finally, non-aggregated and uniform magnetite NPs were only prepared in TREG, which most likely resulted from the better coating effect and the more suitable reaction temperature of TREG. The high reaction temperature of 280 ℃ provides the magnetite NPs with high crystallinity and high magnetization. The cytotoxicity assay indicates that the MIONPs do not affect the viability of cells even when their concentrations are up to 200 mg Fe/L. The TREG coated magnetite NPs synthesized by this method are demonstrated with excellent MRI contrast effect and unusual cancer cellular affinity in vitro experiments, enabling them to be applicable for the cell or molecular imaging and diagnosis of cancer[38]. In fact, the coating layer of polyol is not stable enough to prevent the aggregation of MIONPs over time, so a more stable surface modification is necessary. Zhang et al.[99] synthesized MIONPs via the thermal decomposition of $Fe(acac)_3$ in polyethylene glycol solvent with poly(vinyl pyrrolidone) (PVP) or poly(ethylene imine) (PEI). The colloidal stability of the MIONPs was enhanced due to the coating of PVP or PEI, and their sizes and zeta potentials could be modulated by the coating polymers. The oleylamine coated γ-Fe_2O_3 NPs were prepared through a polyol process with ferrocene as a precursor,

a small amount of 1,2-hexadecandiol as a reducing agent, and the oleylamine as both the solvent and a stabilizer[100]. Hachani et al.[101] systematically studied the process of polyol synthesis by exploring the effects of reaction conditions (i.e., reaction time, type of polyol solvent, and concentration of iron precursor) on the properties of MIONPs including size, morphology, and magnetism. Research results demonstrate that the TREG coated MIONPs have long-term stability and little toxicity to hMSCs after modifying with 3,4-dihydroxyhydrocinnamic acid (DHCA) or tartaric acid (TA). Therefore, they have great potential in the applications of MRI and stem cell tracking. The polyol process usually proceeds by thermal decomposing the $Fe(acac)_3$ in the high-boiling polyols. The as-prepared polyol-modified MIONPs are hydrophilic with high crystallinity, but the long-term stability and size uniformity of the products are not good enough. Although the preparation of MIONPs by the polyol method is easy to scale-up, large amount of organic solvents and expensive precursor are inevitable to be used for such large-scale syntheses[37].

5.3 High-temperature Decomposition Method

High-temperature decomposition method is the best way to synthesize monodisperse MIONPs with high crystallinity, which is mainly carried out in a high-boiling organic solvent by decomposing the organic compounds of iron at a high temperature. The group of Taeghwan synthesized monodisperse MIONPs on an ultra large scale through the thermal decomposition of Fe-oleate complex in high boiling organic solvent. The size of the MIONPs increased from 5 nm to 22 nm with the increase of the boiling temperatures of the organic solvents (as depicted in Fig.8) [33].

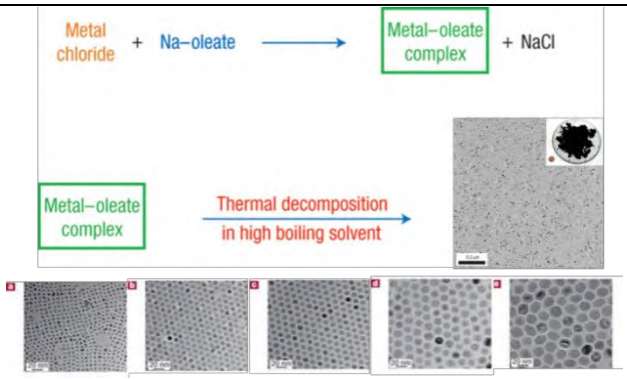

Fig. 8 Ultra large scale synthesis of monodisperse MIONPs with different sizes: (a) 5 nm, using solvent 1-hexadecene (boiling temperature 274 ℃); (b) 9 nm，using solvent octyl ether (boiling temperature 287 ℃); (c) 12 nm，using solvent 1-octadecene (boiling temperature 317 ℃); (d) 16 nm，using solvent 1-eicosene (boiling temperature 330 ℃); (e) 22 nm，using solvent trioctylamine (boiling temperature 365 ℃); (reproduced with permission[33], Copyright 2004, Springer Nature)

The magnetization of superparamagnetic MIONPs increase with increasing particle size, and the T_2 contrast effect usually has the same trend. Besides, the anti-phagocytosis capability is also related to the particle size, which should be considered for their applications in vivo MRI[8,102]. ES-MIONPs are synthesized on a large scale by the same method. One difference is that the oleyl alcohol was used as a capping agent to restrict the growth of MIONPs[103]. The as-synthesized polyethylene glycol-derivatized phosphine oxide (PO-PEG) modified ES-MIONPs possess high r_1 relaxivity and long blood half-time, and they are nontoxic until the concentration is up to 100 mg Fe/ml, so they can be used for the T_1-weighted MRI of various blood vessels. Magnetite NPs with a shape of cube and sizes ranging from 20 to 160 nm were prepared via the decomposition of $Fe(acac)_3$ in benzyl ether in the presence of oleic acid[104]. The PEG-phospholipids coated ferrimagnetic cubic MIONPs with an edge length of 22 nm prepared by this method had a superior T_2 contrast effect. They were reported with the r_2 value of 761 s^{-1} mM^{-1}, which is close to the theoretically predicted value (800 s^{-1} mM^{-1}), and they did not show cytotoxicity at the concentration

up to 0.75 mg Fe/mL, so they can play vital roles in the early diagnosis and detection of tumor metastasis[23]. The concave octapod MIONPs were synthesized by the thermal decomposition of Fe-oleate complex in the mixed solvent of 1-octadecene with small amount of oleic acid and distilled water. The NaCl was added and it played an important role in the formation of octapod shape. As deduced, the chloride ions would selectively bind to the high-index facets of MIONPs and restrict their growth, resulting in the formation of the octapod shape. The octapod MIONPs exhibited higher r_2 value than spherical MIONPs, even though their magnetization was smaller than that of the latter. It is possible that the highly inhomogeneous magnetic field induced by the unique shape of octapod MIONPs caused this phenomenon, and the octapod MIONPs did not show appreciable cytotoxicity for 24 h at the concentration of 0.1 mg Fe/ml[24]. A high-temperature decomposition procedure assisted by microwave heating can produce MIONPs in a short time with a high yield, and the products have higher magnetization, larger specific absorption rate, and higher r_2 value than the similar sized MIONPs prepared by the common thermal decomposition method. Therefore, they can be applied for the MRI contrast agents and cancer magnetic hyperthermia agents[46,105].

Conventional MIONPs show great value as MRI contrast agents, however, their contrast effects are still unsatisfactory compared with fluorescence imaging and positron emission tomography. In order to enhance the signal sensitivity and contrast effect of MRI, MIONPs doped with many other metallic elements were prepared. Lee et al.[106] fabricated monodisperse and highly crystalline MFe_2O_4 (M refers to Mn, Co, or Ni) NPs by the high-temperature reaction between iron tris-2,4-pentadionate and MCl_2 in octyl ether, and the oleic acid and oleyamine were used as surfactants. As shown in Fig.9, different metallic dopants endow the MFe_2O_4 NPs with specific magnetization, magnetic spin structure, magnetic moment, and r_2 value.

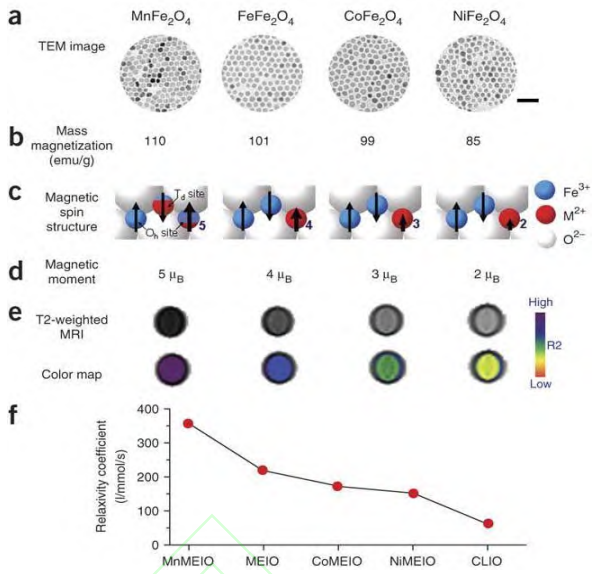

Fig. 9 Properties of MFe_2O_4 (M = Mn, Fe, Co, Ni) nanoparticles: (a) TEM, scale bar 50 nm; (b) mass magnetization; (c) magnetic spin structure; (d) magnetic moment; (e, f) T_2-weighted spin echo MR images and corresponding color maps and relaxivity coefficients (r_2), at 1.5 T (CLIO refers to the MR contrast agent cross-linked iron oxide. Reproduced with permission[106], Copyright 2006, Springer Nature.)

The $(Zn_xMn_{1-x})Fe_2O_4$ NPs and $(Zn_xFe_{1-x})Fe_2O_4$ NPs were prepared by using iron tris-2,4-pentadionate and MCl_2 (M= Zn, Mn, or Fe) as precursors. Among them, $(Zn_{0.4}Mn_{0.6})Fe_2O_4$ NPs and $(Zn_{0.4}Fe_{0.6})Fe_2O_4$ NPs both with size of ~15 nm were reported with extremely high saturation magnetization (Ms) values, 175 emu/g (Zn+Mn+Fe) and 161 emu/g (Zn+Fe) respectively, which far exceeded the Ms value of bulk Fe_3O_4. Compared with conventional MIONPs, their MRI contrast effects increased eight to fourteen times and their hyperthermia effects are enhanced four times. The preliminary in vitro study indicated that they are nontoxic to healthy cells[20]. Different precursors such as $Fe(acac)_3$, $Mn(acac)_3$, and $Zn(acac)_3$ were also used to prepare the Mn-Zn ferrite by a similar method. The morphologies regulation of monodisperse Mn-Zn ferrite NPs from spherical to cubical, star-like, and multi-branched nanoclusters was studied by varying the molar ratio of surfactants oleic acid and oleyamine based on the control of nucleation and growth dynamics[25,107-108]. MIONPs doped with other kinds of

elements like Gd[109] and Eu[110] were prepared by the high-temperature decomposition of corresponding precursors. Both MIONPs and metallic elements doped MIONPs prepared via high-temperature decomposition method possess superior monodispersity, crystallinity, and magnetic properties, but they are usually hydrophobic and need a complicated ligand exchange treatment to transform into aqueous medium before being applied to the physiological environments. Besides, the extensive use of expensive and toxic organic reagents and precursors also restricts their biomedical applications.

6 Modifications and Applications of MIONPs

Iron based magnetic nanomaterials not only possess small size effects, surface effects, and quantum effects belonging to nanomaterials, but also show unique magnetic properties and biological effects. The properties and potential applications of some discussed iron based magnetic nanoparticles are listed in Table 1. Compared with the pure iron NPs and iron based alloy NPs, MIONPs are benign, low toxic, biocompatible, and biodegradable, so they are the only inorganic magnetic nanomaterials approved by the U.S FDA for clinical use at present. Although the biocompatibility and biosafety of MIONPs are much better than other magnetic NPs, the naked MIONPs would also contribute to the cytotoxicity. Therefore, an appropriate surface modification is still necessary to ensure the colloidal stability and biosafety of MIONPs. The surface modification of MIONPs is also an important research subject that much monomeric stabilizers, polymer stabilizers, and inorganic materials such as carboxylates, phosphates, dextran, polyethylene glycol, silica, and gold have been studied to protect and functionalize the MIONPs for better biomedical applications[74,111-112].

Table 1 Properties and potential applications of some referred iron-based magnetic nanoparticles

NPs	Coating materials	Shapes	Sizes (nm)	Preparation methods	Magnetic property	Other properties	Potential applications
amorphous-/bcc-Fe[60]	oleylamine	spherical	~13/12.5	thermal decomposition	~65/84 emu/g NPs	\	magnetic and catalytic
bcc-Fe[63]	oleylamine	spherical	~15	thermal decomposition	~164 emu/g Fe	magnetic heating effect	MRI, magnetic hyperthermia
Fe@Au[62]	CTAB	spherical	~15	reverse micelle	~11.9 emu/g NPs	NIR absorption	drug delivery, PTT
$Fe_{70}Co_{30}$[65]	Polyvinylpyrr-olidone	cubic	~12	physical gas condensation	~226 emu/g	\	magnetic hyperthermia
FeCo[66]	EG	spherical	~30	polyol method	~221 emu/g	\	\
FeCo@ GC[9]	phospholipid–PEG	spherical	~7/4	chemical vapour deposition	~215/162 emu/g	NIR absorption	MRI, PTT, cell labeling, drug release
fcc-FePt[67]	TMAOH	spherical	~9	thermal decomposition	~400 kA/m	\	MRI, magnetic hyperthermia, immunomagnetic cell separation
FePt[69]	cysteamine	spherical	~3/6/12	polyol method	~1.7/3.2/12.3 emu/g Fe	X-ray absorption	MRI/CT, radio frequency-induced hyperthermia
Fe_5C_2[71]	carbon	spherical	~20	thermal decomposition	~125 emu/g	NIR absorption	MRI, PTT, PAT
Fe_3O_4[28]	PAA	spherical	~3.6	coprecipitation	~9.5 emu/g	\	T_1-MRI, pH-responsive drug release
γ-Fe_2O_3[51]	PSC	spherical	~7	coprecipitation	~105 emu/g Fe	\	T_2-MRI

Fe_3O_4[97]	no	spherical	~31.1	hydrothermal	~97.4 emu/g Fe	SQUID-MRX	MRI, SQUID imaging
Fe_3O_4[38]	TREG	spherical	~8	polyol method	~80 emu/g	\	MRI, cancer diagnosis
Fe_3O_4[101]	TREG + DHCA/TA	spherical	~9.1	polyol method	~80 emu/g	\	MRI, stem cell tracking
Fe_3O_4[8]	DMSA	spherical	~4/6/9 /12	thermal decomposition	~25/43/ 80/102 emu/g Fe	\	T_2-MRI, cancer diagnosis
iron oxide[103]	PO-PEG	spherical	~1.5/ 2.2/ 3	thermal decomposition	~3.91/ 83.9/273 μ_B	\	T_1-MRI, diagnosis of the myocardial, renal and vascular diseases
iron oxide[23]	PEG-phospholipids	cubic	~22	thermal decomposition	~106 emu/g Fe	\	T_2-MRI, early diagnosis and detection of tumor metastasis
iron oxide[24]	oleic acid	octapod	edge length ~20/30	thermal decomposition	~51/71 emu/g	\	T_2-MRI, cancer diagnosis, magnetic hyperthermia, magnetically guided drug delivery
(Mn/Fe/Co/Ni)Fe_2O_4[106]	DMSA	spherical	~12	thermal decomposition	~110/ 101/99/85 emu/g	\	T_2-MRI, molecular imaging probe
$(Zn_{0.4}Mn_{0.6})Fe_2O_4$ /$(Zn_{0.4}Fe_{0.6})Fe_2O_4$[20]	DMSA	spherical	~15	thermal decomposition	~175 emu/g (Zn+Mn+Fe) / ~161 emu/g (Zn+Fe)	\	T_2-MRI, magnetic hyperthermia

Remarks: SQUID-MRX refers to the superconducting quantum interference device magnetorelaxometry. Other abbreviations have been noted in the text part. "\" refers to no mentions in the reference, and "/" refers to or.

Most of the MIONPs currently approved in clinical application or testing are coated with carbohydrate. Ferumoxide and Ferucarbotran (generic name), approved as T_2 contrast agents for the indication of liver, spleen, and bone marrow are coated with dextran and carboxy-dextran, respectively. Ferumoxytol (generic name), approved as the intravenous iron supplement for iron deficiency anemia, is coated with PSC[113]. Monomer carboxylate citrate is used as the coating material of the very small MIONPs (VSOP-C184) which have strong T_1 shortening effect and are well suited for the magnetic resonance angiography (MRA)[114]. Although the MIONPs modified with some other materials have not been approved for clinical study, they also have great diagnostic and therapeutic functions. The MIONPs coated with mesoporous silica is a typical instance of multifunctional MIONPs. The fluorescein and drugs can be incorporated into the mesopores of silica shell, so they can be applied to the multimodal imaging of MR and fluorescence imaging as well as drug delivery[115]. Au coated MIONPs can be regarded as a magnetic-plasmonic theranostic platform which can realize the MR, photoacoustic, and positron emission tomography multimodal imaging and the photothermal therapy of cancer[116-117]. In order to reduce the influences of serum proteins and mitigate the uptake of phagocytic cells, the hydrophilic PEG can be coated on the MIONPs to increase their circulation time. Morever, some targeting ligands, such as antibodies, folic acid, and peptides were modified on the surface of MIONPs to increase their active targeting functions to tumors, because the passive target by the enhanced permeability and retention (EPR) effect or magnetically targeting of MIONPs are usually not efficient

enough[118].

7 Summary and Remarks

In addition to good biocompatibility and biosafety, a kind of ideal magnetic nanomaterials for clinical application should have narrow size distribution, high crystallinity, excellent magnetic properties, and can be fabricated on a large scale. At present, the existing preparation methods are not very suitable for preparing MIONPs with good properties for clinical demands. Hydrothermal method is a simple way to synthesize MIONPs with good crystallinity without the use of organic solvent, but the size and shape uniformities and dispersity of their products seem to be bad. The sol-gel method is simple and economical, but the purity of their products is not ideal. The polyol method can easily prepare water disperse MIONPs with more uniform size and good crystallinity, but the process requires a great number of organic solvents and expensive precursors. High-temperature decomposition method is the best way to synthesize monodisperse MIONPs with high crystallinity, but the hydrophobic products need a complicated ligand exchange treatment to transform into aqueous medium, and the synthesis process also consumes plenty of expensive and toxic organic reagents and precursors. Among all of the methods, chemical co-precipitation method is the simplest and commonest strategy to prepare MIONPs for biomedical applications, but the particle size distribution and crystallinity of the products need further improvement.

The development of MIONPs preparation methods is not only significant to the nanomaterial industry, butalso closely related to the development of clinical magnetic nano-drug for diagnosis and treatment. The development of the synthesis methods is mainly dependent on the understanding and improving of the synthesis mechanism. Although the specific formation mechanism of MIONPs is not fully clear, our understanding to it is becoming deeper and deeper as the development of advanced characterization and preparation techniques. Through constant innovation and improvement, MIONPs and many other magnetic nanomaterials will certainly demonstrate their clinical value.

References

[1] Li Y, Chen Z W, Gu N. *In vitro* biological effects of magnetic nanoparticles. Chinese Science Bulletin, 2012, 57(31): 3972-3978. DOI: 10.1007/s11434-012-5295-8.

[2] Kwon Y M, Xia Z, Glyn-Jones S, et al. Dose-dependent cytotoxicity of clinically relevant cobalt nanoparticles and ions on macrophages *in vitro*. Biomedical Materials, 2009, 4(2):025018. DOI: 10.1088/ 1748-6041/4/2/025018.

[3] Magaye R, Zhao J S, Bowman L, et al. Genotoxicity and carcinogenicity of cobalt-, nickel- and copper-based nanoparticles (Review). Experimental and Therapeutic Medicine, 2012, 4(4): 551-561. DOI: 10.3892/etm. 2012.656.

[4] Ling T, Xie L, Zhu J, et al. Icosahedral face-centered cubic Fe nanoparticles: Facile synthesis and characterization with aberration-corrected TEM. Nano Letters, 2009, 9(4): 1572-1576. DOI: 10.1021/nl8037294.

[5] Peng S, Wang C, Xie J, et al. Synthesis and stabilization of monodisperse Fe nanoparticles. Journal of the American Chemical Society, 2006, 128(33): 10676-10677. DOI: 10.1021/ja063969h.

[6] Huang S H, Juang R S. Biochemical and biomedical applications of multifunctional magnetic nanoparticles: A review. Journal of Nanoparticle Research, 2011, 13: 4411-4430. DOI: 10.1007/s11051-011-0551-4.

[7] Wu L H, Mendoza-Garcia A, Li Q, et al. Organic phase syntheses of magnetic nanoparticles and their applications. Chemical Reviews, 2016, 116(18): 10473-10512. DOI: 10.1021/acs.chemrev.5b00687.

[8] Jun Y W, Huh Y M, Choi J S, et al. Nanoscale size effect of magnetic nanocrystals and their utilization for cancer diagnosis via magnetic resonance imaging. Journal of the American Chemical Society, 2005, 127(16): 5732-5733. DOI: 10.1021/ja0422155.

[9] Seo W S, Lee J H, Sun X M, et al. FeCo/graphitic-shell nanocrystals as advanced magnetic-resonance-imaging

and near-infrared agents. Nature Materials, 2006, 5: 971-976. DOI: 10.1038/nmat1775.

[10] Zheng W P, Rong Z, Gao F P, et al. Folate-conjugated magnetic nanoparticles for tumor hyperthermia therapy: *In Vitro* and *In Vivo* studies. Journal of Nanoscience and Nanotechnology, 2016, 16(8): 8352-8359. DOI: 10.1166/jnn.2016.12622.

[11] Clay N, Baek K, Shkumatov A, et al. Flow-mediated stem cell labeling with superparamagnetic iron oxide nanoparticle clusters. ACS Applied Materials & Interfaces, 2013, 5(20): 10266-10273. DOI: 10.1021/am4030998.

[12] Hayashi K, Sato Y, Sakamoto W, et al. Theranostic nanoparticles for MRI-guided thermochemotherapy: "Tight" clustering of magnetic nanoparticles boosts relaxivity and heat-generation power. ACS Biomaterials Science & Engineering, 2017, 3(1): 95-105. DOI: 10.1021/acsbiomaterials.6b00536.

[13] Yoon T J, Yu K N, Kim E, et al. Specific targeting, cell sorting, and bioimaging with smart magnetic silica core-shell nanomaterials. Small, 2006, 2(2): 209-215. DOI: 10.1002/smll.200500360.

[14] Gao L Z, Zhuang J, Nie L, et al. Intrinsic peroxidase-like activity of ferromagnetic nanoparticles. Nature Nanotechnology, 2007, 2: 577-583. DOI: 10.1038/nnano.2007.260.

[15] Chen Z W, Yin J J, Zhou Y T, et al. Dual enzyme-like activities of iron oxide nanoparticles and their implication for diminishing cytotoxicity. ACS Nano, 2012, 6(5): 4001-4012. DOI: 10.1021/nn300291r.

[16] Song L N, Huang C, Zhang W, et al. Graphene oxide-based Fe_2O_3 hybrid enzyme mimetic with enhanced peroxidase and catalase-like activities. Colloids and Surfaces A: Physicochemical and Engineering Aspects, 2016, 506: 747-755. DOI: 10.1016/j.colsurfa.2016.07.037.

[17] Gao L Z, Fan K L, Yan X Y. Iron oxide nanozyme: A multifunctional enzyme mimetic for biomedical applications. Theranostics, 2017, 7(13): 3207-3227. DOI: 10.7150/thno.19738.

[18] Ma M, Xie J, Zhang Y, et al. Fe_3O_4@Pt nanoparticles with enhanced peroxidase-like catalytic activity. Materials Letters, 2013, 105: 36-39. DOI: 10.1016/j.matlet. 2013.04.020.

[19] Lee J H, Kim J W, Cheon J. Magnetic nanoparticles for multi-imaging and drug delivery. Molecules and Cells, 2013, 35(4): 274-284. DOI: 10.1007/s10059-013-0103-0.

[20] Jang J T, Nah H, Lee J H, et al. Critical enhancements of MRI contrast and hyperthermic effects by dopant-controlled magnetic nanoparticles. Angewandte Chemie International Edition, 2009, 48(7): 1234-1238. DOI: 10.1002/anie.200805149.

[21] Gossuin Y, Gillis P, Hocq A, et al. Magnetic resonance relaxation properties of superparamagnetic particles. Wiley Interdisciplinary Reviews: Nanomedicine and Nanobiotechnology, 2009, 1(3): 299-310. DOI: 10.1002/wnan.36.

[22] Pöselt E, Kloust H, Tromsdorf U, et al. Relaxivity optimization of a PEGylated iron-oxide-based negative magnetic resonance contrast agent for T_2-weighted spin-echo imaging. ACS Nano, 2012, 6(2): 1619-1624. DOI: 10.1021/nn204591r.

[23] Lee N, Choi Y, Lee Y, et al. Water-dispersible ferrimagnetic iron oxide nanocubes with extremely high *r*(2 relaxivity for highly sensitive in vivo MRI of tumors. Nano Letter, 2012, 12(6): 3127-3131. DOI: 10.1021/nl3010308.

[24] Zhao Z H, Zhou Z J, Bao J F, et al. Octapod iron oxide nanoparticles as high-performance T_2 contrast agents for magnetic resonance imaging. Nature Communications, 2013, 4: Article number: 2266. DOI: 10.1038/Ncomms3266.

[25] Xie J, Yan C Z, Zhang Y, et al. Shape evolution of "multibranched" Mn-Zn ferrite nanostructures with high performance: A transformation of nanocrystals into nanoclusters. Chemistry of Materials, 2013, 25(18): 3702-3709. DOI: 10.1021/cm402036d.

[26] Song M J, Zhang Y, Hu S L, et al. Influence of morphology and surface exchange reaction on magnetic properties of monodisperse magnetite nanoparticles. Colloids and Surfaces A: Physicochemical and Engineering Aspects, 2012, 408: 114-121. DOI: 10.1016/j.colsurfa.2012.05.039.

[27] Li Z, Tan B, Allix M, et al. Direct coprecipitation route to monodisperse dual-functionalized magnetic iron oxide nanocrystals without size selection. Small, 2008,

4(2): 231-239. DOI: 10.1002/smll.200700575.

[28] Shen Z, Chen T, Ma X, et al. Multifunctional theranostic nanoparticles based on exceedingly small magnetic iron oxide nanoparticles for T_1-weighted magnetic resonance imaging and chemotherapy. ACS Nano, 2017, 11(11): 10992-11004. DOI: 10.1021/acsnano.7b04924.

[29] Daou T J, Pourroy G, Bégin-Colin S, et al. Hydrothermal synthesis of monodisperse magnetite nanoparticles. Chemistry of Materials, 2006, 18(18): 4399-4404. DOI: 10.1021/cm060805r.

[30] Peng J H, Hojamberdiev M, Xu Y H, et al. Hydrothermal synthesis and magnetic properties of gadolinium-doped $CoFe_2O_4$ nanoparticles. Journal of Magnetism and Magnetic Materials, 2011, 323(1): 133-137. DOI: 10.1016/j.jmmm.2010.08.048.

[31] Pascal C, Pascal J L, Favier F, et al. Electrochemical synthesis for the control of γ-Fe_2O_3 nanoparticle size. Morphology, microstructure, and magnetic behavior. Chemistry of Materials, 1999, 11(1): 141-147. DOI: 10.1021/Cm980742f.

[32] Starowicz M, Starowicz P, Żukrowski J, et al. Electrochemical synthesis of magnetic iron oxide nanoparticles with controlled size. Journal of Nanoparticle Research, 2011, 13(12): 7167-7176. DOI: 10.1007/s11051-011-0631-5.

[33] Park J, An K J, Hwang Y S, et al. Ultra-large-scale syntheses of monodisperse nanocrystals. Nature Materials, 2004, 3: 891-895. DOI: 10.1038/nmat1251.

[34] Kim D, Lee N, Park M, et al. Synthesis of uniform ferrimagnetic magnetite nanocubes. Journal of the American Chemical Society, 2009, 131(2): 454-455. DOI: 10.1021/ja8086906.

[35] Masthoff I C, Kraken M, Menzel D, et al. Study of the growth of hydrophilic iron oxide nanoparticles obtained via the non-aqueous sol-gel method. Journal of Sol-Gel Science and Technology, 2016, 77(3): 553-564. DOI: 10.1007/s10971-015-3883-1.

[36] Masthoff I C, Kraken M, Mauch D, et al. Study of the growth process of magnetic nanoparticles obtained via the non-aqueous sol-gel method. Journal of Materials Science, 2014, 49(14): 4705-4714. DOI: 10.1007/s10853-014-8160-0.

[37] Cai W, Wan J Q. Facile synthesis of superparamagnetic magnetite nanoparticles in liquid polyols. Journal of Colloid and Interface Science, 2007, 305(2): 366-370. DOI: 10.1016/j.jcis.2006.10.023.

[38] Wan J, Cai W, Meng X, et al. Monodisperse water-soluble magnetite nanoparticles prepared by polyol process for high-performance magnetic resonance imaging. Chemical Communications, 2007, (47): 5004-5006. DOI: 10.1039/b712795b.

[39] Lee Y J, Lee J W, Bae C J, et al. Large-scale synthesis of uniform and crystalline magnetite nanoparticles using reverse micelles as nanoreactors under reflux conditions. Advanced Functional Materials, 2005, 15(12): 503-509. DOI: 10.1002/adfm.200590040.

[40] Gotić M, Jurkin T, Musić S. Factors that may influence the micro-emulsion synthesis of nanosize magnetite particles. Colloid and Polymer Science, 2007, 285(7): 793-800. DOI: 10.1007/s00396-006-1624-2.

[41] Ali R, Khan M A, Mahmood A, et al. Structural, magnetic and dielectric behavior of $Mg_{1-x}Ca_xNi_yFe_{2-y}O_4$ nano-ferrites synthesized by the micro-emulsion method. Ceramics International, 2014, 40: 3841-3846. DOI: 10.1016/j.ceramint.2013.08.024.

[42] Shen L Z, Qiao Y S, Guo Y, et al. Facile co-precipitation synthesis of shape-controlled magnetite nanoparticles. Ceramics International, 2014, 40(1): 1519-1524. DOI: 10.1016/j.ceramint.2013.07.037.

[43] Lin Y L, Wei Y, Sun Y H, et al. Synthesis and magnetic characterization of magnetite obtained by monowavelength visible light irradiation. Materials Research Bulletin, 2012, 47(3): 614-618. DOI: 10.1016/j.materresbull.2011.12.042.

[44] Feng J, Mao J, Wen X G, et al. Ultrasonic-assisted in situ synthesis and characterization of superparamagnetic Fe_3O_4 nanoparticles. Journal of Alloys and Compounds, 2011, 509(37): 9093-9097. DOI: 10.1016/j.jallcom.2011.06.053.

[45] Abu Mukh-Qasem R, Gedanken A. Sonochemical synthesis of stable hydrosol of Fe_3O_4 nanoparticles. Journal of Colloid and Interface Science, 2005, 284(2): 489-494. DOI: 10.1016/j.jcis.2004.10.073.

[46] Liang Y J, Zhang Y, Guo Z R, et al. Ultrafast preparation of monodisperse Fe_3O_4 nanoparticles by microwave-assisted thermal decomposition. Chemistry - A European Journal, 2016, 22(33): 11807-11815. DOI: 10.1002/chem.201601434.

[47] Kalyani S, Sangeetha J, Philip J. Microwave assisted synthesis of ferrite nanoparticles: Effect of reaction temperature on particle size and magnetic properties. Journal of Nanoscience and Nanotechnology, 2015, 15(8): 5768-5774. DOI: 10.1166/jnn.2015.10274.

[48] Vereda F, de Vicente J, Hidalgo-Álvarez R. Influence of a magnetic field on the formation of magnetite particles via two precipitation methods. Langmuir, 2007, 23(7): 3581-3589. DOI: 10.1021/la0633583.

[49] Wang J, Chen Q, Zeng C, et al. Magnetic-field-induced growth of single-crystalline Fe_3O_4 nanowires. Advanced Materials, 2004, 16(2): 137-140. DOI: 10.1002/adma.200306136.

[50] Chen B, Li Y, Zhang X Q, et al. An efficient synthesis of ferumoxytol induced by alternating-current magnetic field. Materials Letters, 2016, 170: 93-96. DOI: 10.1016/j.matlet.2016.02.006.

[51] Chen B, Sun J F, Fan F G, et al. Ferumoxytol of ultrahigh magnetization produced by hydrocooling and magnetically internal heating co-precipitation. Nanoscale, 2018, 10: 7369-7376. DOI: 10.1039/c8nr00736e.

[52] Fang M, Strȍm V, Olsson R T, et al. Particle size and magnetic properties dependence on growth temperature for rapid mixed co-precipitated magnetite nanoparticles. Nanotechnology, 2012, 23(14): 145601. DOI: 10.1088/0957-4484/23/14/145601.

[53] LaMer V K, Dinegar R H. Theory, production and mechanism of formation of monodispersed hydrosols. Journal of the American Chemical Society, 1950, 72(11): 4847-4854. DOI: 10.1021/Ja01167a001.

[54] Vreeland E C, Watt J, Schober G B, et al. Enhanced nanoparticle size control by extending LaMer's mechanism. Chemistry of Materials, 2015, 27(17): 6059-6066. DOI: 10.1021/acs.chemmater.5b02510.

[55] Baghbanzadeh M, Carbone L, Cozzoli P D, et al. Microwave-assisted synthesis of colloidal inorganic nanocrystals. Angewandte Chemie International Edition, 2011, 50(48): 11312-11359. DOI: 10.1002/anie.201101274.

[56] Erdemir D, Lee A Y, Myerson A S. Nucleation of crystals from solution: Classical and two-step models. Accounts of Chemical Research, 2009, 42(5): 621-629. DOI: 10.1021/ar800217x.

[57] Baumgartner J, Dey A, Bomans P H H, et al. Nucleation and growth of magnetite from solution. Nature Materials, 2013, 12: 310-314. DOI: 10.1038/NMAT3558.

[58] Yang C, Wu J J, Hou Y L. Fe_3O_4 nanostructures: synthesis, growth mechanism, properties and applications. Chemical Communications, 2011, 47: 5130-5141. DOI: 10.1039/C0cc05862a.

[59] Feld A, Weimer A, Kornowski A, et al. Chemistry of shape-controlled iron oxide nanocrystal formation. ACS Nano, 2019, 13(1): 152-162. DOI: 10.1021/acsnano.8b05032.

[60] Zhang S, Jiang G M, Filsinger G T, et al. Halide ion-mediated growth of single crystalline Fe nanoparticles. Nanoscale, 2014, 6: 4852-4856. DOI: 10.1039/c4nr00193a.

[61] Singh G, Kumar P A, Lundgren C, et al. Tunability in crystallinity and magnetic properties of core-shell Fe nanoparticles. Particle & Particle Systems Characterization, 2014, 31(10): 1054-1059. DOI: 10.1002/ppsc.201400032.

[62] Kayal S, Ramanujan R V. Anti-cancer drug loaded iron-gold core-shell nanoparticles (Fe@Au) for magnetic drug targeting. Journal of Nanoscience and Nanotechnology, 2010, 10(9): 5527-5539. DOI: 10.1166/jnn.2010.2461.

[63] Lacroix L M, Huls N F, Ho D, et al. Stable single-crystalline body centered cubic Fe nanoparticles. Nano Letters, 2011, 11(4): 1641-1645. DOI: 10.1021/nl200110t.

[64] Lu L Y, Zhang W T, Wang D, et al. Fe@Ag core-shell nanoparticles with both sensitive plasmonic properties and tunable magnetism. Materials Letters, 2010, 64(15): 1732-1734. DOI: 10.1016/j.matlet.2010.04.025.

[65] Jing Y, Sohn H, Kline T, et al. Experimental and theoretical investigation of cubic FeCo nanoparticles for magnetic hyperthermia. Journal of Applied Physics, 2009,

105(7): 07B305. DOI: 10.1063/1.3074136.

[66] Zamanpour M, Chen Y J, Hu B L, et al. Large-scale synthesis of high moment FeCo nanoparticles using modified polyol synthesis. Journal of Applied Physics, 2012, 111(7): 07B528. DOI: 10.1063/1.3677773.

[67] Maenosono S, Suzuki T, Saita S. Superparamagnetic FePt nanoparticles as excellent MRI contrast agents. Journal of Magnetism and Magnetic Materials, 2008, 320(9): L79-L83. DOI: 10.1016/j.jmmm.2008.01.026.

[68] Liu F, Zhu J, Yang W, et al. Building nanocomposite magnets by coating a hard magnetic core with a soft magnetic shell. Angewandte Chemie International Edition, 2014, 53(8): 2176-2180. DOI: 10.1002/anie.201309723.

[69] Chou S W, Shau Y H, Wu P C, et al. In vitro and in vivo studies of FePt nanoparticles for dual modal CT/MRI molecular imaging. Journal of the American Chemical Society, 2010, 132(38): 13270-13278. DOI: 10.1021/ja1035013.

[70] Yang C, Zhao H B, Hou Y L, et al. Fe_5C_2 nanoparticles: A facile bromide-induced synthesis and as an active phase for Fischer-Tropsch synthesis. Journal of the American Chemical Society, 2012, 134(38): 15814-15821. DOI: 10.1021/ja305048p.

[71] Yu J, Yang C, Li J D S, et al. Multifunctional Fe_5C_2 nanoparticles: A targeted theranostic platform for magnetic resonance imaging and photoacoustic tomography-guided photothermal therapy. Advanced Materials, 2014, 26(24): 4114-4120. DOI: 10.1002/adma.201305811.

[72] Wang X, Zhang P, Wang W, et al. Magnetic N-enriched Fe_3C/graphitic carbon instead of Pt as an electrocatalyst for the oxygen reduction reaction. Chemistry - A European Journal, 2016, 22(14): 4863-4869. DOI: 10.1002/chem.201505138.

[73] Ling D S, Hyeon T. Chemical design of biocompatible iron oxide nanoparticles for medical applications. Small, 2013, 9(9-10): 1450-1466. DOI: 10.1002/smll.201202111.

[74] Laurent S, Forge D, Port M, et al. Magnetic iron oxide nanoparticles: Synthesis, stabilization, vectorization, physicochemical characterizations, and biological applications. Chemical Reviews, 2008, 108(6): 2064-2110. DOI: 10.1021/cr068445e.

[75] Ahn T, Kim J H, Yang H M, et al. Formation pathways of magnetite nanoparticles by coprecipitation method. Journal of Physical Chemistry C, 2012, 116(10): 6069-6076. DOI: 10.1021/jp211843g.

[76] Massart R. Preparation of aqueous magnetic liquids in alkaline and acidic media. IEEE Transactions on Magnetics, 1981, 17(2): 1247-1248. DOI: 10.1109/Tmag.1981.1061188.

[77] Roth H C, Schwaminger S P, Schindler M, et al. Influencing factors in the co-precipitation process of superparamagnetic iron oxide nano particles: A model based study. Journal of Magnetism and Magnetic Materials, 2015, 377: 81-89. DOI: 10.1016/j.jmmm.2014.10.074.

[78] Aphesteguy J C, Kurlyandskaya G V, de Celis J P, et al. Magnetite nanoparticles prepared by co-precipitation method in different conditions. Materials Chemistry and Physics, 2015, 161: 243-249. DOI: 10.1016/j.matchemphys.2015.05.044.

[79] Gnanaprakash G, Mahadevan S, Jayakumar T, et al. Effect of initial pH and temperature of iron salt solutions on formation of magnetite nanoparticles. Materials Chemistry and Physics, 2007, 103(1): 168-175. DOI: 10.1016/j.matchemphys.2007.02.011.

[80] Bai C, Jia Z Y, Song L N, et al. Time-dependent T_1-T_2 switchable magnetic resonance imaging realized by c(RGDyK) modified ultrasmall Fe_3O_4 nanoprobes. Advanced Functional Materials, 2018, 28:1802281. DOI: 10.1002/Adfm.201802281.

[81] Chen L, Xie J, Wu H A, et al. Improving sensitivity of magnetic resonance imaging by using a dual-targeted magnetic iron oxide nanoprobe. Colloids and Surfaces B: Biointerfaces, 2018, 161: 339-346. DOI: 10.1016/j.colsurfb.2017.10.059.

[82] Ma M, Wu Y, Zhou J, et al. Size dependence of specific power absorption of Fe_3O_4 particles in AC magnetic field. Journal of Magnetism and Magnetic Materials, 2004, 268(1-2): 33-39. DOI: 10.1016/S0304-8853(03)00426-8.

[83] Ma M, Zhang Y, Yu W, et al. Preparation and characterization of magnetite nanoparticles coated by amino silane. Colloids and Surfaces A: Physicochemical

and Engineering Aspects, 2003, 212(2-3): 219-226. DOI: 10.1016/S0927-7757(02)00305-9.

[84] Wu Y H, Song M J, Xin Z, et al. Ultra-small particles of iron oxide as peroxidase for immunohistochemical detection. Nanotechnology, 2011, 22(22): 225703. DOI: 10.1088/0957-4484/22/22/225703.

[85] Wang C Y, Hong J M, Chen G, et al. Facile method to synthesize oleic acid-capped magnetite nanoparticles. Chinese Chemical Letters, 2010, 21(2): 179-182. DOI: 10.1016/j.cclet.2009.10.024.

[86] Hassan A A, Sandre O, Cabuil V, et al. Synthesis of iron oxide nanoparticles in a microfluidic device: Preliminary results in a coaxial flow millichannel. Chemical Communications, 2008, 15: 1783-1785. DOI: 10.1039/b719550h.

[87] Kumar K, Nightingale A M, Krishnadasan S H, et al. Direct synthesis of dextran-coated superparamagnetic iron oxide nanoparticles in a capillary-based droplet reactor. Journal of Materials Chemistry, 2012, 22: 4704-4708. DOI: 10.1039/c2jm30257h.

[88] Li Y, Hu K, Chen B, et al. Fe_3O_4@PSC nanoparticle clusters with enhanced magnetic properties prepared by alternating-current magnetic field assisted co-precipitation. Colloids and Surfaces A: Physicochemical and Engineering Aspects, 2017, 520: 348-354. DOI: 10.1016/j.colsurfa.2017.01.073.

[89] Ma M, Zhang Y, Shen X L, et al. Targeted inductive heating of nanomagnets by a combination of alternating current (AC) and static magnetic fields. Nano Research, 2015, 8(2): 600-610. DOI: 10.1007/s12274-015-0729-7.

[90] Camponeschi E, Walker J, Garmestani H, et al. Surfactant effects on the particle size of iron (III) oxides formed by sol-gel synthesis. Journal of Non-Crystalline Solids, 2008, 354(34): 4063-4069. DOI: 10.1016/j.jnoncrysol.2008.04.018.

[91] Cui H T, Liu Y, Ren W Z. Structure switch between α-Fe_2O_3, γ-Fe_2O_3 and Fe_3O_4 during the large scale and low temperature sol-gel synthesis of nearly monodispersed iron oxide nanoparticles. Advanced Powder Technology, 2013, 24(1): 93-97. DOI: 10.1016/j.apt.2012.03.001.

[92] Zhang Y, Cao J X, Nie D P, et al. Preparation and characterization of nanometer iron oxide by sol-gel method and supercritical fluid drying technology. Key Engineering Materials, 2008, 368-372: 617-619. DOI: 10.4028/www.scientific.net/KEM.368-372.617.

[93] Li J C, Shi X Y, Shen M W. Hydrothermal synthesis and functionalization of iron oxide nanoparticles for MR imaging applications. Particle & Particle Systems Characterization, 2014, 31(12): 1223-1237. DOI: 10.1002/ppsc.201400087.

[94] Cai H D, An X, Cui J, et al. Facile hydrothermal synthesis and surface functionalization of polyethyleneimine-coated iron oxide nanoparticles for biomedical applications. ACS Applied Materials & Interfaces, 2013, 5(5): 1722-1731. DOI: 10.1021/am302883m.

[95] Takami S, Sato T, Mousavand T, et al. Hydrothermal synthesis of surface-modified iron oxide nanoparticles. Materials Letters, 2007, 61(26): 4769-4772. DOI: 10.1016/j.matlet.2007.03.024.

[96] Hu L, Percheron A, Chaumont D, et al. Microwave-assisted one-step hydrothermal synthesis of pure iron oxide nanoparticles: magnetite, maghemite and hematite. Journal of Sol-Gel Science and Technology, 2011, 60: 198-205. DOI: 10.1007/s10971-011-2579-4.

[97] Ge S, Shi X, Sun K, et al. Facile hydrothermal synthesis of iron oxide nanoparticles with tunable magnetic properties. Journal of Physical Chemistry C, 2009, 113(31): 13593-13599. DOI: 10.1021/jp902953t.

[98] Ozel F, Kockar H, Karaagac O. Growth of iron oxide nanoparticles by hydrothermal process: Effect of reaction parameters on the nanoparticle size. Journal of Superconductivity and Novel Magnetism, 2015, 28(3): 823-829. DOI: 10.1007/s10948-014-2707-9.

[99] Zhang B L, Tu Z J, Zhao F Y, et al. Superparamagnetic iron oxide nanoparticles prepared by using an improved polyol method. Applied Surface Science, 2013, 266(1): 375-379. DOI: 10.1016/j.apsusc.2012.12.032.

[100] Yamada Y, Shimizu R, Kobayashi Y. Iron oxide and iron carbide particles produced by the polyol method. Hyperfine Interactions, 2016, 237: 6. DOI: 10.1007/S10751-016-1220-X.

[101] Hachani R, Lowdell M, Birchall M, et al. Polyol

synthesis, functionalisation, and biocompatibility studies of superparamagnetic iron oxide nanoparticles as potential MRI contrast agents. Nanoscale, 2016, 8: 3278-4395. DOI: 10.1039/c5nr03867g.

[102] Chen L, Xie J, Wu H A, et al. Precise study on size-dependent properties of magnetic iron oxide nanoparticles for in vivo magnetic resonance imaging. Journal of Nanomaterials, 2018,2018: Article ID 3743164. DOI: 10.1155/2018/3743164.

[103] Kim B H, Lee N, Kim H, et al. Large-scale synthesis of uniform and extremely small-sized iron oxide nanoparticles for high-resolution T_1 magnetic resonance imaging contrast agents. Journal of the American Chemical Society, 2011, 133(32): 12624-12631. DOI: 10.1021/ja203340u.

[104] Kim D, Lee N, Park M, et al. Synthesis of uniform ferrimagnetic magnetite nanocubes. Journal of the American Chemical Society, 2009, 131(2): 454-455. DOI: 10.1021/ja8086906.

[105] Liang Y J, Fan F G, Ma M, et al. Size-dependent electromagnetic properties and the related simulations of Fe_3O_4 nanoparticles made by microwave-assisted thermal decomposition. Colloids and Surfaces A: Physicochemical and Engineering Aspects, 2017, 530: 191-199. DOI: 10.1016/j.colsurfa.2017.06.059.

[106] Lee J H, Huh Y M, Jun Y, et al. Artificially engineered magnetic nanoparticles for ultra-sensitive molecular imaging. Nature Medicine, 2007, 13: 95-99. DOI: 10.1038/nm1467.

[107] Xie J, Yan C Y, Yan Y, et al. Multi-modal Mn-Zn ferrite nanocrystals for magnetically-induced cancer targeted hyperthermia: A comparison of passive and active targeting effects. Nanoscale, 2016, 8: 16902-16915. DOI: 10.1039/c6nr03916b.

[108] Xie J, Zhang Y, Yan C Y, et al. High-performance PEGylated Mn-Zn ferrite nanocrystals as a passive-targeted agent for magnetically induced cancer theranostics. Biomaterials, 2014, 35(33): 9126-9136. DOI: 10.1016/j.biomaterials.2014.07.019.

[109] Zhang G L, Du R H, Zhang L L, et al. Gadolinium-doped iron oxide nanoprobe as multifunctional bioimaging agent and drug delivery system. Advanced Functional Materials, 2015, 25(38): 6101-6111. DOI: 10.1002/adfm.201502868.

[110] Yang L J, Zhou Z J, Liu H Y, et al. Europium-engineered iron oxide nanocubes with high T_1 and T_2 contrast abilities for MRI in living subjects. Nanoscale, 2015, 7: 6843-6850. DOI: 10.1039/c5nr00774g.

[111] Tian X, Zhang L H, Yang M, et al. Functional magnetic hybrid nanomaterials for biomedical diagnosis and treatment. Wiley Interdisciplinary Reviews: Nanomedicine and Nanobiotechnology, 2018, 10(1):e1476. DOI: 10.1002/Wnan.1476.

[112] Zhu K, Ju Y, Xu J, et al. Magnetic nanomaterials: Chemical design, synthesis, and potential applications. Accounts of Chemical Research, 2018, 51(2): 404-413. DOI: 10.1021/acs.accounts.7b00407.

[113] Ittrich H, Peldschus K, Raabe N, et al. Superparamagnetic iron oxide nanoparticles in biomedicine: Applications and developments in diagnostics and therapy. Fortschr Röntgenstr, 2013, 185(12): 1149-1166. DOI: 10.1055/s-0033-1335438.

[114] Taupitz M, Wagner S, Schnorr J, et al. Phase I clinical evaluation of citrate-coated monocrystalline very small superparamagnetic iron oxide particles as a new contrast medium for magnetic resonance imaging. Investigative Radiology, 2004, 39(7): 394-405. DOI: 10.1097/01.rli.0000129472.45832.b0.

[115] Kim J, Kim H S, Lee N, et al. Multifunctional uniform nanoparticles composed of a magnetite nanocrystal core and a mesoporous silica shell for magnetic resonance and fluorescence imaging and for drug delivery. Angewandte Chemie - International Edition, 2008, 47(44): 8438-8441. DOI: 10.1002/anie.200802469.

[116] Ji X J, Shao R P, Elliott A M, et al. Bifunctional gold nanoshells with a superparamagnetic iron oxide-silica core suitable for both MR imaging and photothermal therapy. Journal of Physical Chemistry C, 2007, 111(17): 6245-6251. DOI: 10.1021/jp0702245.

[117] Lin L S, Yang X Y, Zhou Z J, et al. Yolk-shell nanostructure: An ideal architecture to achieve harmonious integration of magnetic-plasmonic hybrid theranostic platform. Advanced Materials, 2017, 29: 1606681. DOI: 10.1002/Adma.201606681.

[118] Wei J, Shuai X Y, Wang R, et al. Clickable and imageable multiblock polymer micelles with magnetically guided and PEG-switched targeting and release property for precise tumor theranosis. Biomaterials, 2017, 145: 138-153. DOI: 10.1016/j.biomaterials.2017.08.005.